# Submerged and non-submerged 3D bioprinting approaches for the fabrication of complex structures with the hydrogel pair alginate/methylcellulose and GelMA

Huijun Li,[1] Yu Jun Tan,[2] Raj Kiran,[3] Shu Beng Tor,[1] Kun Zhou*,[1]

[1]*Singapore Centre for 3D Printing, School of Mechanical and Aerospace Engineering, Nanyang Technological University, 50 Nanyang Avenue, Singapore 639798, Singapore*

[2]*Institute for Health Innovation & Technology, National University of Singapore, 117599 Singapore*

[3]*School of Mechanical and Aerospace Engineering, Nanyang Technological University, 50 Nanyang Avenue, Singapore 639798, Singapore*

**Abstract**

Submerged and non-submerged three-dimensional (3D) bioprinting approaches are demonstrated for successful printing of complex hydrogel structures using a pair of polyelectrolyte hydrogels including the polyanionic alginate/methylcellulose (Alg/MC) and the polycationic gelatin methacrylate (GelMA). For the submerged approach, the cell-GelMA mixture is printed within Alg/MC, which serves as a temporary supporting material during printing. This approach can be utilized for fabrication of complex structures with increasing complexity rather than simple ones. For the non-submerged approach, the Alg/MC and cell-GelMA are printed alternately for fabrication of structures. Due to its high viscosity, the Alg/MC is printed first to form the base layer which provides support to the subsequent cell-GelMA layer, as Alg/MC can rapidly solidify after printing but for cell-GelMA mixture it is difficult to maintain its shape without the post-crosslinking. For both approaches, the structures obtained are exposed to UV light only once after printing to strengthen the printed structures, which overcomes the limitations of utilizing GelMA for bioprinting. Before the UV treatment, the electrostatic interactions between Alg/MC and GelMA could efficiently prevent the spreading of hydrogel during the printing process. Both approaches enable the fabrication of structures with good shape fidelity and structural integrity. Additionally, good biocompatibility is achieved by printing of this hydrogel pair with cell viability above 93% up to 5 days. This work opens up many opportunities in 3D bioprinting including a wide range of diverse hydrogels for printing and a great potential for fabrication of complex cell-laden hydrogel structures with increasing complexities.

**Keywords**: extrusion, hydrogel, submerged, alginate, methylcellulose, GelMA

* Corresponding author. E-mail addresses: kzhou@ntu.edu.sg (K. ZHOU)

## 1. Introduction

Three-dimensional (3D) printing technologies with suitable biomaterials provide the opportunity to print artificial tissues or organs in a layer-by-layer fashion through computer-aided manufacturing [1-3]. The bioprinting approaches [4, 5] include extrusion-based [6-9], inkjet-based [10], and laser-assisted printing [11]. Extrusion-based printing is one of the most commonly used technologies owing to its advantage like ease of deposition of highly viscous bioinks (viscosity ~$6\times10^7$ mPa·s) [5, 12] and high efficiency.

Hydrogels are the widely used biomaterials for extrusion-based bioprinting due to their superior biocompatibility and hydrated 3D matrices for cell encapsulation. The hydrogels used for extrusion-based printing should possess shear thinning properties for ease of extrusion through the fine nozzle. Also, they should rapidly solidify after extruding out from the nozzle to maintain their own shapes and even support the subsequently printed layers to be stacked on top of them. Hence, it is very difficult to stack soft hydrogel onto a 3D structure as even a small deformation in the lower layers of a printed structure can result in dissatisfactory print. Thus, there is still a need of biocompatible hydrogels with good printability for fabrication of 3D structures with accurate geometries [13].

Natural hydrogels (e.g., alginate [14, 15], collagen [16], gelatin [17, 18], and chitosan [19, 20]) are commonly used for biofabrication but they are a class of hydrogels consisting of polysaccharides or proteins which makes it difficult to employ them for creating fine, complex and large scale 3D structures [21]. Towards this end, synthetic hydrogels can be considered as potential candidates for bioprinting as they have tailorable mechanical properties but some of them are chemically cross-linked through severe ultraviolet (UV) crosslinking or chemical crosslink processes which lead to a reduction in biocompatibility [22, 23]. Gelatin methacrylate (GelMA) is a commonly used synthetic hydrogels for bioprinting [24]. The traditional method for printing GelMA is utilizing UV treatment to crosslink the GelMA chains covalently after printing each

GelMA layer, which may lead to the repeated curing of the few bottom layers and a reduction in the cell viability [22, 23]. Thus, the development in the bioinks is still in need of significant improvement in the field of 3D bioprinting.

To achieve the aim of printing hydrogel structures with good shape fidelity, two methods for extrusion-based bioprinting have been reported: extrusion of self-support hydrogels with rapid solidification in air [25-27], and support bath assisted printing [21, 28, 29]. For the first method, the extruded hydrogels should be solidified quickly through different stimuli (e.g., UV radiation or thermal gelation) [26, 27]. The highly viscous hydrogels with shear-thinning and thixotropic properties are commonly utilized for this method. However, a high shear stress is needed to extrude the viscous hydrogels through the narrow nozzles which may affect the cell viability in the hydrogels. For the hydrogels with low viscosities, such as GelMA, UV treatment is required after printing each layer but this printing process has potential harm on cells [30, 31]. On the other hand, in the second method, a support bath with a strengthening medium is required to support the printed hydrogel structures. Moreover, the supporting material should be easily removed after printing in order to obtain the printed object. Only limited hydrogels are available for fabrication of hydrogel structures through using the second method [21, 28, 29].

For both methods, all the special criteria (e.g., rheological, mechanical and biological adaptation) for the hydrogels and technologies for bioprinting should be met to prevent damage to the printed structures and harm on the cells, which results in only limited hydrogels available for successful bioprinting of 3D hydrogel structures. Additionally, the complexity of the printed hydrogel based structures remain limited, although some simple structures (e.g., square lattices) can be printed [21]. Thus, the development of the bioinks and the improvement in the 3D bioprinting technologies for fabrication of complex hydrogel structures with living cells remains challenging.

In this study, Alg/MC and GelMA as a pair of bioinks with the aid of two promising approaches (submerged and non-submerged printing) are proposed for printing of complex cell-

laden hydrogel structures. For the submerged printing, the suspended cell-GelMA mixture is printed in the Alg/MC hydrogel which serves as a temporary supporting material during printing. For the non-submerged printing, the highly viscous Alg/MC hydrogel blend and the cell-GelMA mixture are printed alternately to obtain the cell-laden structures. For both approaches, the UV cross-linking of GelMA could further strengthen the whole printed structure after printing. The effectiveness of GelMA and Alg/MC as a pair of bioinks are examined in terms of mechanical property, structural integrity and biocompatibility.

## 2. Materials and Methods

### *2.1 Hydrogel preparation*

Sodium Alg was purchased from Sigma-Aldrich (Singapore) and its guluronic acid block content was 50-60%. The Alg powder was added in the Dulbecco's phosphate-buffered saline (DPBS) solution. The obtained mixture was stirred magnetically at room temperature for 12 h. The prepared Alg hydrogel with various concentrations (3, 6, 9, 12 wt %) was named Alga, corresponding to the Alg concentration of a% (wt/wt) in the DPBS solutions. Then, the Alg/MC blend was prepared according to the literature [26]. Briefly, the MC powder (MW ~ 88 kDa, Sigma-Aldrich, Singapore) was added gradually to the Alg hydrogel (~ 80 $^{o}$C). Finally, the Alg/MC blend was obtained after stirring the mixture thoroughly and then slowly cooling it to room temperature. The Alga/MCb corresponds to the weight of Alg and MC in the blend at a ratio of a:b (wt/wt). In this study, the concentrations of MC (b wt %) in the blend will be 1, 3, 6, 9 and 12 wt %. The bioinks utilized for this study can be classified into 5 groups: MC1 group (Alg3/MC1, Alg6/MC1, Alg9/MC1 and Alg12/MC1), MC3 group (Alg3/MC3, Alg6/MC3, Alg9/MC3 and Alg12/MC3), MC6 group (Alg3/MC6, Alg6/MC6, Alg9/MC6 and Alg12/MC6), MC9 group (Alg3/MC9, Alg6/MC9, Alg9/MC9 and Alg12/MC9), and MC12 group (Alg3/MC12, Alg6/MC12, Alg9/MC12 and Alg12/MC12).

The GelMA was synthesized as per the steps followed in the literature [32]. Briefly, 10 g of gelatin powder (type A from porcine skin, Sigma-Aldrich, Singapore) was added into 100 mL DPBS solution while stirring. Methacrylic anhydride (MA) (Sigma-Aldrich, Singapore) with a volume of 0.7 mL was gradually added to gelatin hydrogel while the mixture was magnetically stirred for 4 hours (~50 $^{o}$C). The obtained mixture was dialyzed at 37 $^{o}$C for 7 days against deionized water. Thereafter, the solution was freeze dried for 7 days. In this study, only GelMA10 (10 wt% GelMA) was prepared due to its superior printability than other concentrations as concluded form previous study [33]. The photo initiator Irgacure 2959 was purchased from Sigma-Aldrich (Singapore). It was added to the GelMA hydrogel maintaining a ratio of 0.01 g: 4.5 mL.

*2.2 Material characterization*

One-layer grids were printed and investigated to estimate the printability of a hydrogel. Printability $P_r$ of a hydrogel could be estimated by [34]

$$P_r = \frac{L^2}{16A} \tag{1}$$

where $L$ and $A$ are the perimeter and area of one lattice in the printed structure, respectively, and can be determined by the ImageJ software.

Transmittance spectra for Alg9/MC1, Alg9/MC6 and Alg9/MC9 were measured by a Shimadzu spectrophotometer (Shimadzu 1800) in the 300-700 nm light spectrum.

A rotational rheometer (DHR, TA Instruments, USA) with a parallel plate geometry of 40 mm in diameter and a measurement gap of 0.55 mm, was used to investigate the rheological properties of the hydrogels. Alg9/MC1, Alg9/MC6 and Alg9/MC9 were investigated at room temperature of 26 $^{o}$C. The recovery tests were conducted in three steps to estimate the rheological properties of a hydrogel before, during, and after the extrusion process. During step I, a low shear rate (~0.1 $s^{-1}$) was applied on the Alg/MC hydrogel for 60 s to simulate the initial condition of Alg/MC before a nozzle was moving through it. Step II simulated the state of Alg/MC hydrogel while a nozzle was

moving through the Alg/MC. A high shear rate (~100 $s^{-1}$) was applied on the hydrogels for 10 s. During step III, the shear rate was decreased to 0.1 $s^{-1}$ again and held for 60 s to imitate the final state of Alg/MC after extrusion.

The degree of methacrylation (DM) of GelMA used in this study was determined by $^{1}H$ nuclear magnetic resonance (NMR) spectroscopy (AV300 NMR). Details of this measurement have been provided in Supporting Information.

*2.3 3D bioprinting of hydrogel structures*

For bioprinting, the pyrex bottles, nozzles and syringes were autoclaved before preparation of hydrogels. The GelMA solutions at 37 $^{o}C$ were sterile-filtered through a membrane of 0.2 μm before usage. The temperature for printing hydrogel structure is around 26 $^{o}C$ which is the working temperature of the bioprinter (BioFactory bioprinter machine, RegenHU).

*2.3.1 3D bioprinting of hydrogel structures using the non-submerged approach*

Here, multilayered grids with living cells were printed by extrusion the Alg9/MC9 from one syringe, followed by extrusion the cell-GelMA10 mixture from the other syringe. The Alg/MC blend and cell-GelMA mixture were printed alternately, which resulted in a 3D structure named Alg/MC-GelMA, as demonstrated in **Fig. 1a**. After the structures were fully printed, they were exposed to UV light for 10 s in a UV flood (Shuttered UV system, Epoxy and equipment technology Pte Ltd). It is noted that the inner diameter of the nozzles for printing was 0.25 mm and each sample used for mechanical testing, structural integrity investigation and cell viability measurement had 20 layers.

*2.3.2 3D bioprinting of hydrogel structures using the submerged approach*

The support bath consisted of Alg/MC hydrogel, which provided temporary support for the intended 3D structures. The Alg/MC blend was poured into a petri dish before printing. Alg9/MC1,

Alg9/MC6 and Alg9/MC9 were prepared to compare their feasibilities of using as bath materials. The 3D model for printing was designed using SolidWorks software. All stereolithography (STL) files were processed by the software (STL converter) on the bioprinter. The pre-designed 3D model was sliced into 0.25 mm thick layers to generate G-code instructions to control the continuous extrusion of hydrogels. Thereafter, the prepared GelMA hydrogel was poured into a syringe and then capped with a nozzle (diameter: 0.25 mm).

In this study, a 3D flower was printed to demonstrate the advantages of this approach. The GelMA and cells mixture was extruded within the Alg/MC bath at a designed position to create the first petal, followed by printing of the other identical petals one by one in the bath. The printed structure can be further solidified through exposing it to UV light for 10 s in the UV flood. Finally, the complete printed part was released from the support bath by soaking it in a large beaker (1L) filled with DPBS at 37 $^{o}$C along with supporting material. Gentle mechanical agitation could efficiently remove Alg/MC hydrogel. The procedure for bioprinting of a GelMA construct within a supporting bath is illustrated in **Fig. 1b**. Similar to the non-submerged approach, each sample used for mechanical testing, structural integrity investigation and cell viability measurement had 20 layers along thickness.

*2.4 Mechanical testing of the bioprinted samples*

The tensile tests were carried out using a uniaxial tensile tester (Instron 5569, UK) with a 100 N load cell at room temperature. Alg9/MC9 and GelMA10 were used for printing the dumbbell-shaped samples. The freshly printed dumbbell-shaped samples were 15 mm in length, 5 mm in width and 5 mm in thickness. Before testing, the printed Alg/MC-GelMA and GelMA tensile bars were cured in a UV flood for different time duration of 10 s and 60 s. A loading rate of 0.025 mm $s^{-1}$ was utilized for all the tensile tests. The elastic modulus was determined from the slope of the linear region (0 to 10% of the strain range) of the stress-strain curves.

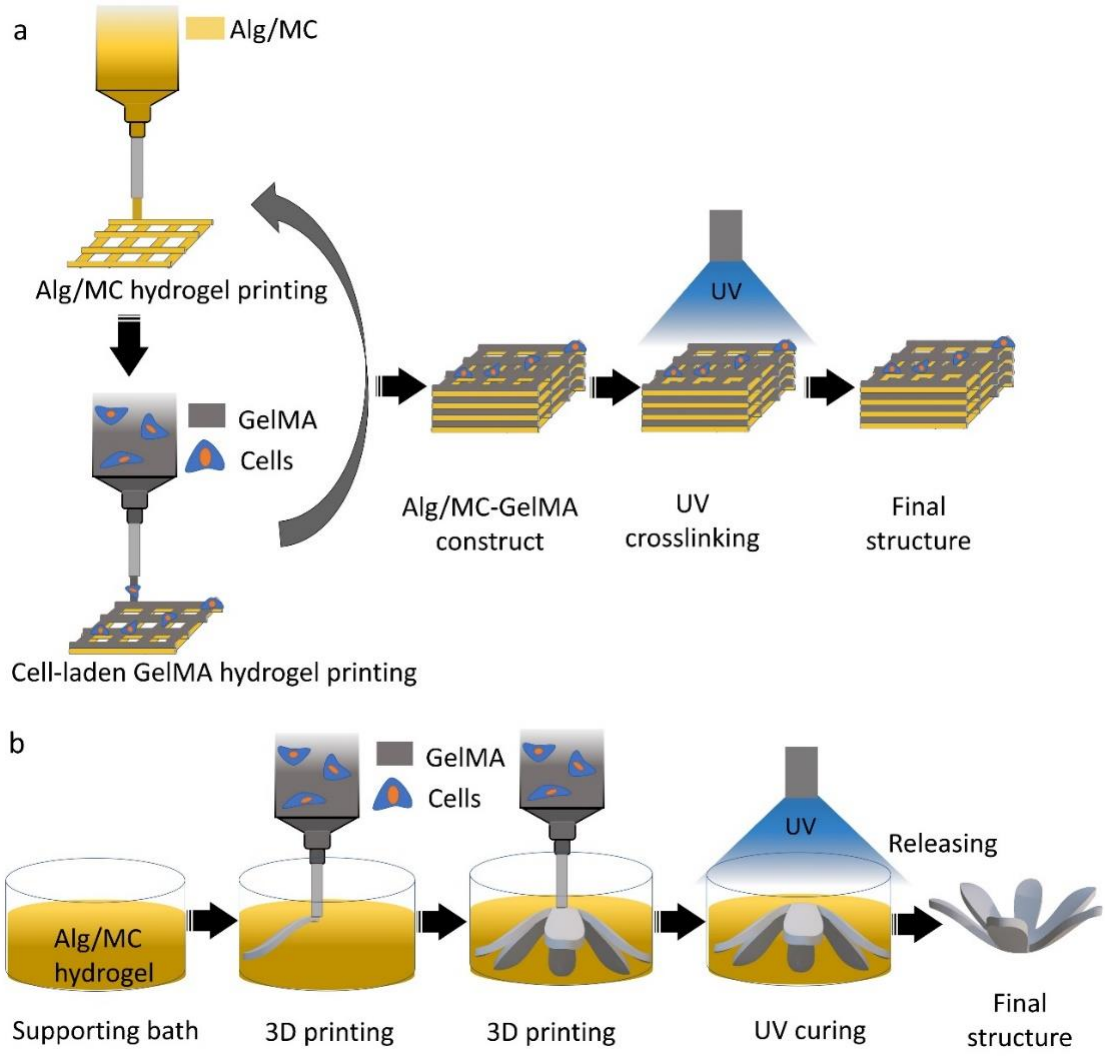


**Fig. 1**. Schematics of the procedures for printing of cell-laden hydrogel structures using: (a) the non-submerged approach where the Alg/MC hydrogel and cell-GelMA mixture are printed alternately to obtain an Alg/MC-GelMA structure followed by UV curing of the printed structure only once; (b) the submerged approach where the cell-GelMA mixture is printed in a support bath consisting of Alg/MC hydrogel and cured under UV once completely printed followed by the removal of the support material.

*2.5 Structural integrity of the bioprinted samples*

The Alg/MC-GelMA grids and GelMA flowers were printed through utilizing the non-submerged and submerged printing, respectively. The samples were soaked in DPBS in an incubator at 37 $^{o}$C to investigate their structural integrity over 30 days. The structures solely printed using Alg9/MC9 were also tested as control.

*2.6 Cell viability for the bioprinted samples*

Cells (mouse myoblasts C2C12) were used for bioprinting. Cells were cultured in the Dulbecco's modified Eagle's medium (Sigma-Aldrich, Singapore) supplemented with 1% antibiotic-antimycotic and 10% fetal bovine serum (Sigma-Aldrich, Singapore), in an incubator under 5% $CO_2$ at 37 °C [35]. Thereafter, the cells were mixed with the GelMA10 hydrogel to achieve a final cell density of ~$3.66 \times 10^5$ cells $mL^{-1}$ in the mixture. According to the proposed methodologies, the printed hydrogel structures were obtained and then cultured in the culture medium for 5 days in an incubator (5% $CO_2$ at 37 $^oC$).

Cell viability on the printed construct was determined using a live/dead assay (Molecular Probes). The constructs were incubated for 15 min in a staining solution before investigation through an inverted fluorescence microscopy (Carl Zeiss Axio Vert. A1). The staining solution was prepared with propidium iodide (5 μM) and calcein acetoxymethyl ester (2 μM). C2C12 was also transferred to tissue culture polystyrene (TCPS) and cultured for 5 days as control.

## 3. Results

*3.1 Determination of the optimal composition of Alg/MC blend for the non-submerged approach*

There are a few criteria for selecting or developing a hydrogel suitable for extrusion-based printing: (1) hydrogel should exhibit thixotropic property for rapidly recovering its shear-reduced viscosity after printing in order to maintain the printed shape without excessive flow; (2) the shape of a printed 3D structure should conform to the pre-designed pattern; (3) the hydrogel is required to have a good morphology (i.e., without bubbles).

For the pre-designed grids pattern (square shape), the $P_r$ of an ideal hydrogel should be close to one according to equation (1). **Fig. 2** shows the $P_r$ of each hydrogel blend with different

compositions. For MC1 hydrogels (the concentration of MC was 1 wt %, while the concentration of Alg was varied from 3 to 12 wt %), these hydrogel blends could not form a grid structure with regular shape and square holes as some of the filaments almost fused together. The $P_r$ for the MC1 hydrogels was found to be below one indicating the poor printability of bioinks. Hydrogels with higher Alg concentrations (> 12 wt %) for 1 wt% MC were not prepared for the following reasons: (1) adding more Alg could not significantly improve the printability of the Alg/MC blend as the viscosity of an Alg/MC blend was mainly contributed by MC, which was reported in our previous study [26]; (2) the homogeneous Alg/MC hydrogel blend was not feasible to obtain after adding MC powder to the viscous Alg hydrogel. Hence, Alg/MC hydrogels with higher Alg concentrations (> 12 wt %) were not further considered.

Upon increasing the MC concentrations from 1 wt% to 9 wt%, $P_r$ of the Alg/MC blends increased from 0.85 to 1. However, small bubbles were observed in the Alg12/MC9 during the preparation process, which was attributed to the fact that the Alg12 hydrogel had a high viscosity and thus could not be used to dissolve MC9 powder thoroughly. The shapes of the printed grids using Alg3/MC9, Alg6/MC9, and Alg9/MC9 all highly conformed to the pre-designed pattern, wherein each printed filament had a high resolution and regularity. All the three hydrogels exhibited the shear thinning and thixotropic properties which are the desired properties for extrusion-based printing (**Fig. S1**, Supporting Information). In this work, Alg9/MC9 was selected for further extrusion-based printing as Alg9 can provide more negative ions than Alg3 and Alg6 to form the electrostatic interactions with GelMA.

**Fig. 2e** puts forward the Alg/MC blends with different $P_r$. Most importantly, those blends with excellent printability ($P_r$ ~1) were highlighted in green. This information serves as a guideline for preparing and developing Alg/MC blend for extrusion-based 3D bioprinting.

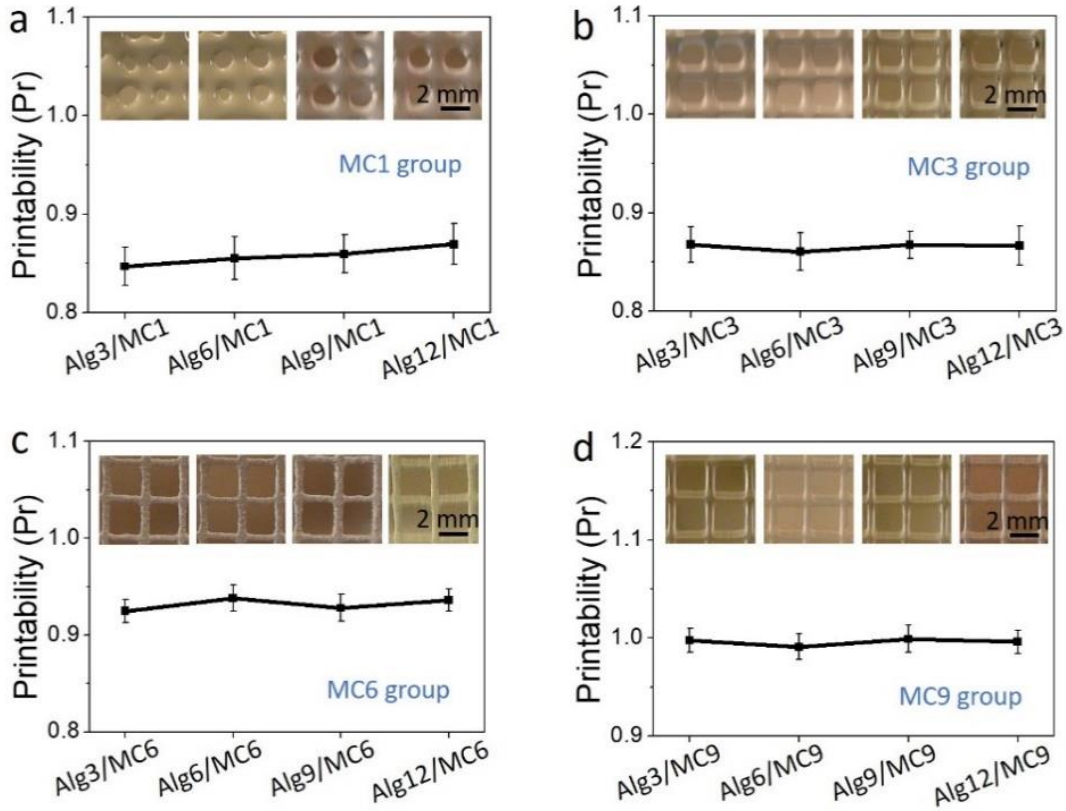


e

| Alg \ MC | 1 | 3 | 6 | 9 | 12 |
|---|---|---|---|---|---|
| 3 | - | - | - | + | X |
| 6 | - | - | - | + | X |
| 9 | - | - | - | + | X |
| 12 | - | - | - | - | X |

+ Excellent printability (High resolution)

- Poor printability (Low resolution)

- Poor printability (Hydrogels with bubbles)

X Not printable (Hydrogels with bubbles and quite infeasible to be extruded out even under the maximum pressure)

**Fig. 2**. Evaluation of $P_r$ for each hydrogel blend with different compositions: (a) $P_r$ for MC1 group; (b) $P_r$ for MC3 group; (c) $P_r$ for MC6 group; (d) $P_r$ for MC9 group and (e) summary table for bioinks selection where the preferable compositions of Alg/MC blend with excellent printability are highlighted in green. The insets in (a-d) show the printed one-layer lattices with different $P_r$.

*3.2 Determination of the optimal composition of Alg/MC blend for the submerged approach*

Criteria for selecting a hydrogel as the support material are as follows: (1) the Alg/MC hydrogel should be transparent which could help the embedded GelMA to form cross-links under UV curing; (2) the Alg/MC hydrogel should support the suspended GelMA to create a pre-designed pattern.

**Fig. 3a** shows the transparency for the Alg9/MC1, Alg9/MC6, and Alg9/MC9. They were all highly transparent (transmittance above 70%) in the range of 315-400 nm, which was the wavelength of the used UV flood. It is to be highlighted that with the high transparency, photo-crosslinks can be formed in GelMA after UV curing.

**Fig. 3b** demonstrates that the tested Alg/MC samples have shear thinning and recovery properties. The shear thinning property could help the printing nozzle easily move through Alg/MC hydrogel due to the shear reduced viscosity of Alg/MC. This property is much more critical for submerged printing, as the movement of the nozzle in the Alg/MC could not cause dragging of the previously printed layers which might distort the whole printed structure. Afterwards, the shear-reduced viscosity of Alg/MC could be rapidly recovered once the shear force was removed. This behavior helps the supporting material Alg/MC to support the suspended GelMA in the designed position. Additionally, the Alg9/MC1, Alg9/MC6 and Alg9/MC9 were compared against their viability of being used as support material. The Alg9/MC1 hydrogel blend had a low viscosity which could not maintain the shape of the printed GelMA after embedding it within Alg9/MC1 bath. In contrast, Alg9/MC9 was too viscous resulting in a longer time for releasing the printed GelMA structure from the Alg9/MC9. Thus, the Alg9/MC6 was used as the support material in this work.

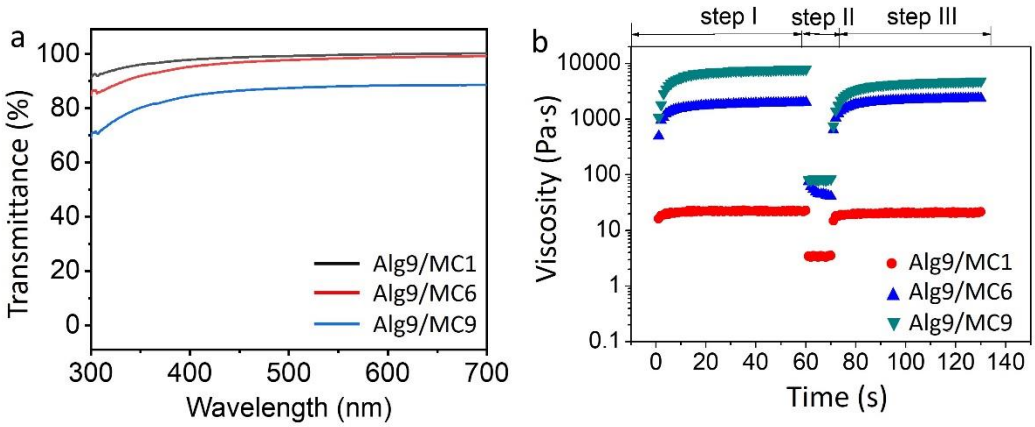


**Fig. 3**. Material characterizations for the tested samples: (a) transmittance spectra for samples and (b) shear shinning and recovery behavior of each sample. Step I represents the state of the hydrogel before nozzle movement while step II and III simulate the state during and after the nozzle movement through Alg/MC hydrogel, respectively.

*3.3 Determination of DM of GelMA*

Gelatin presents cationic nature due to the presence of lysine and arginine residues on gelatin chain [36]. According to the result of $^{1}$H NMR spectra (**Fig. S2**, Supporting Information), the DM of GelMA used here was about 30% which indicated about 30% methylene in lysine groups participated in the reaction with MA to form GelMA [32], and the remaining 70% of the methylene in lysine reveals the cationic nature of GelMA.

*3.4 3D bioprinting of hydrogel structures*

*3.4.1 3D bioprinting of hydrogel structures using the non-submerged approach*

Depositing hydrogels into a construct with high aspect ratio is a well-known challenge. Hence, the height of a printed structure is a direct indication of the stackability and the printability of a bioink. A 10-layered thin-wall structure (**Fig. 4**) was printed by alternate extrusion of Alg/MC and GelMA. The pair of bioinks exhibited an excellent stackability as the pre-designed pattern was

nicely maintained with excellent regularity. The width of each printed filament conforms to the diameter of the used nozzle (0.25 mm). Constructs with 25 layers and 50 layers were also fabricated as illustrated in **Fig. 4**. The final height of this 50-layer construct was around 12 mm. The shape of the printed construct was stable, and the delicate internal porous structure was printed successfully.

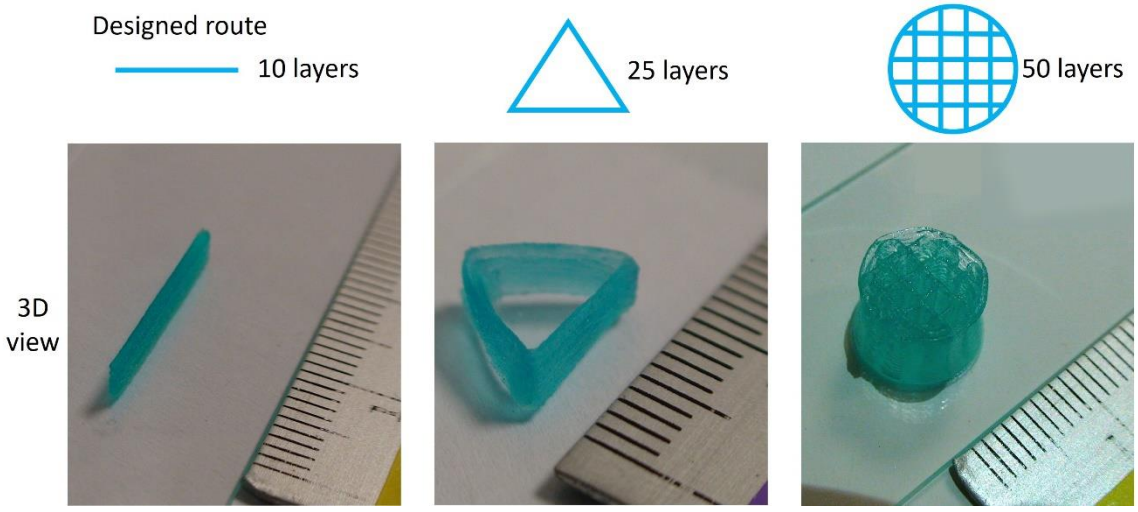


**Fig. 4**. Structures are obtained using non-submerged approach. A 2D structure with 10 layers (height is about 3 mm), a 3D triangle structure with 25 layers (height is about 6 mm) and a 3D grid structure with 50 layers (height is about 12 mm) are demonstrated. Hydrogels are stained with blue-colored food dye for ease of illustration.

*3.4.2 3D bioprinting of hydrogel structures using the submerged approach*

**Fig. 5a** shows the pre-designed 3D model for printing and **Fig. 5b** demonstrates the procedure of printing of a suspended flower (GelMA was stained with orange-colored food dye) in the supporting material. After printing the structure, the post UV-crosslinking could efficiently strengthen the printed structure as Alg/MC was highly transparent (**Fig. 3a**). Finally, the printed object was released from Alg/MC by soaking them in a DPBS solution under subtle mechanical agitation. This approach enables successful printing of complex structure that is consistent with the initial designed 3D model. Additionally, Alg/MC can provide the negatively charged ions, which can form polyelectrolyte complexes with the positively charged GelMA, as illustrated in **Fig. 5c**.

The electrostatic interactions could efficiently prevent the spreading of soft hydrogel during the layer-by-layer printing process which was helpful to stabilize the printed soft structure.

The submerged approach also illustrates an obvious advantage. It can print the hydrogel structures with increasing complexity which could not be fabricated by using the non-submerged printing approach.

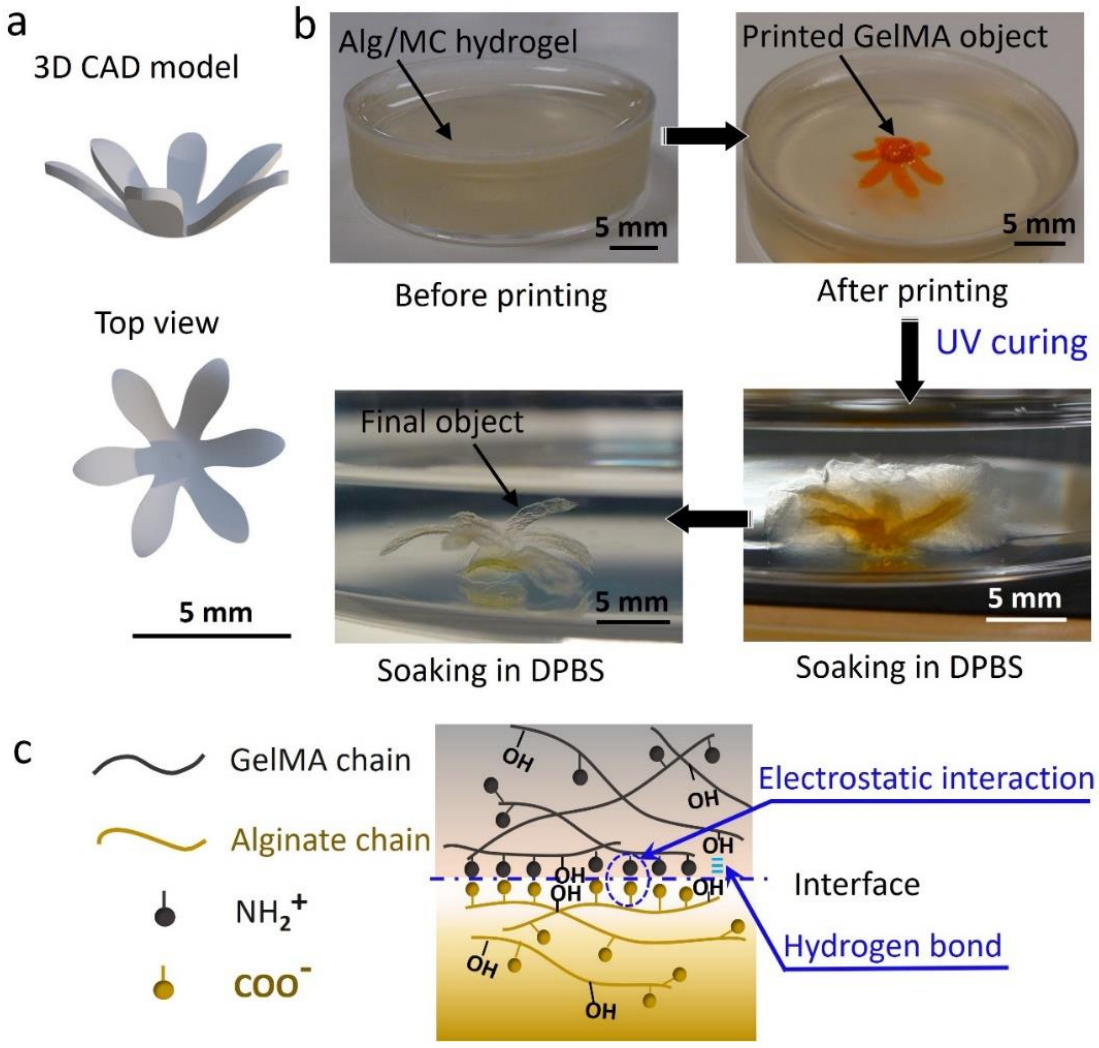


**Fig. 5**. Submerged approach for printing of a 3D flower: (a) Schematic representation of the pre-designed 3D model for printing; (b) demonstration of the procedure of obtaining a 3D GelMA flower and (c) schematic illustration of the interaction between Alg/MC and GelMA.

*3.5 Mechanical testing of the bioprinted samples*

The 3D printed dumbbell-shaped sample for tensile testing is shown in **Fig. 6a**. The representative images of the specimen at the initial state before tensile loading and the deformed state being stretched are shown in **Fig. 6b**. The effect of UV time on mechanical properties of samples was investigated (**Fig. 6c**). The average tensile moduli of the printed Alg/MC-GelMA (UV 10 s), Alg/MC-GelMA (UV 60 s), GelMA (UV 10 s), and GelMA (UV 60 s) were found to be 12.21, 32.91, 14.95 and 37.26 kPa respectively.

In this work, the printed tensile bars were too soft for the tensile test when the UV curing time was less than 10 s. Hence, 10 s was selected as the UV curing time to investigate the structural integrity and cell viability of the bioprinted structures. Therefore, it shows a possibility that the mechanical properties [24], the structural integrity and cell viability of a printed structure may be controlled by adjusting the time for UV curing.

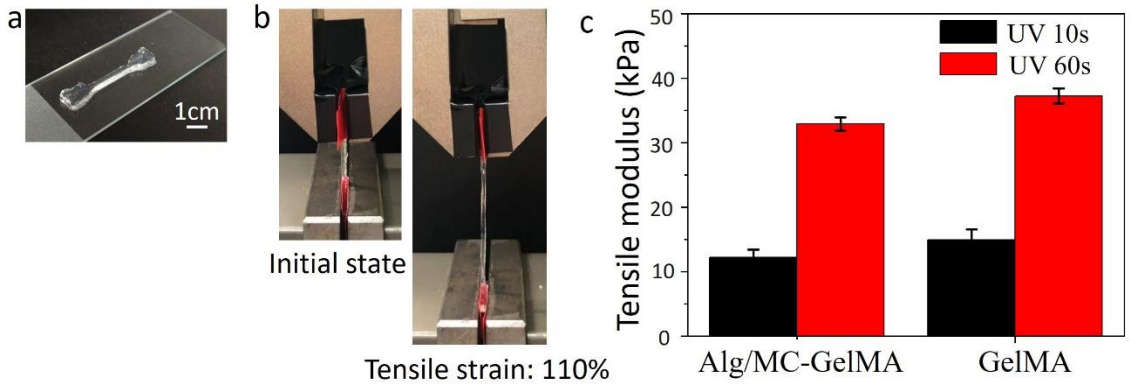


**Fig. 6.** (a) The Alg/MC-GelMA sample printed with exposure to UV for the duration of 60 s; (b) the initial state of the printed sample before tensile loading and its deformed state under the tensile strain of 110%; (c) effects of the UV duration on the tensile moduli of the printed samples.

*3.6 Structural integrity of the bioprinted samples*

Grid structures were printed using the non-submerged approach. **Fig. 7a** shows the representative images of the printed Alg/MC and Alg/MC-GelMA grids in 37 $^{o}$C DPBS solution

over time. The printed Alg/MC construct started to crack on day 3, and the sample broke into several small pieces on day 10. After 30 days of incubation in DPBS, the Alg/MC construct was found to be completely dissolved. As compared to the Alg/MC construct, the printed Alg/MC-GelMA construct exhibited a good structural integrity, where the shape of the printed Alg/MC-GelMA structure could be well maintained for 15 days. However, the Alg/MC-GelMA construct was found to be broken into three pieces by day 20 and completely shattered into small pieces on day 30.

A complex 3D flower was obtained through submerged printing. This printed flower could maintain its shape for about 5 days, as shown in **Fig. 7b**. Thereafter, the structure was gradually degraded and completely dissolved by day 30. Moreover, during the observation time, the soft suspended flower can bend and undulate as water flows past its petals when soaking in a water bath.

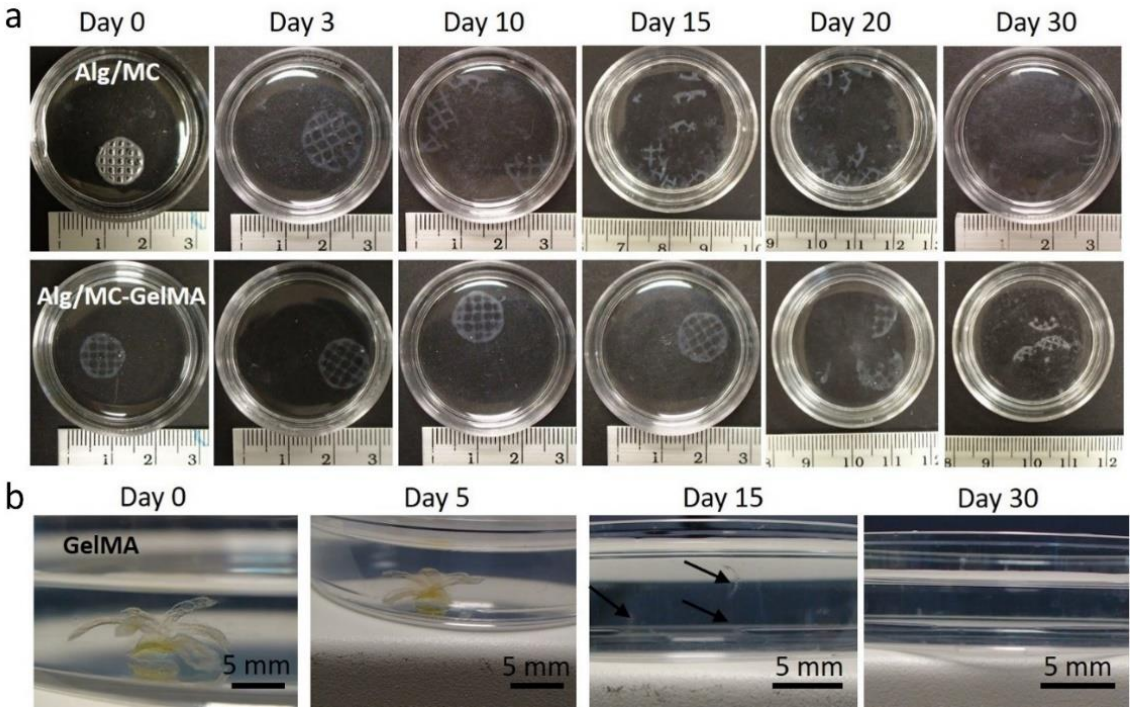


**Fig. 7**. Images for demonstration of the structural integrities of the printed structures in DPBS for different times at 37 °C: (a) structures are obtained using non-submerged approach and (b) 3D flower is printed through using the submerged approach. At day 15, the remaining hydrogel pieces are highlighted using arrows.

*3.7 Cell viability for the bioprinted samples*

**Fig. 8a** demonstrates the representative fluorescent images for the printed Alg/MC-GelMA constructs during culturing. On day 0 and day 5 of culturing, the cell viability of the bioprinted constructs was above 96%, which showed a comparable value to that of the TCPS control, as shown in **Fig. 8b**. The optical microscopy (OM) image of the bioprinted construct was captured immediately after fresh printing of the structure (**Fig. 8c**). The fine filaments (diameter ~0.25 mm) and regular shape could be observed. In addition, the fluorescent images for the living cells on day 0 and day 5 (**Fig. 8a**) demonstrated the morphologies of C2C12 in the printed Alg/MC-GelMA construct. On day 0, the cells had circular morphology in the Alg/MC-GelMA construct while on day 5, almost all the cells showed the spreading and elongating morphologies.

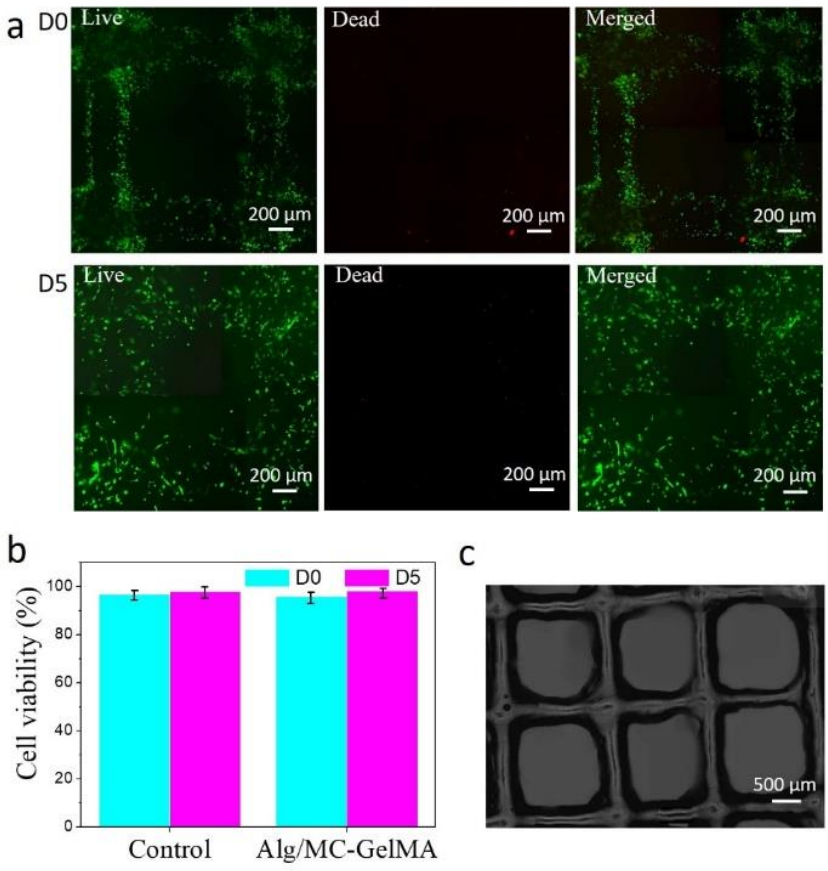


**Fig. 8**. Cell viability for non-submerged printing: (a) fluorescent images for the printed Alg/MC-GelMA structure; (b) cell viability of the bioprinted Alg/MC-GelMA and the control; (c) OM image for the bioprinted structure.

The merged fluorescent images for the live and dead cells in the bioprinted GelMA constructs are demonstrated in **Fig. 9a**. Only limited dead cells were observed during the observation time (5 days). **Fig. 9b** shows that the cell viability of the bioprinted constructs is above 93% during culturing, which showed a comparable value to that of the TCPS control. From **Fig. 9c**, it is evident that the cells were rounded on day 0 in the printed construct. The cell morphologies on the construct indicated the cells were elongated on day 5. All the above findings verify that the bioprinted constructs using these two proposed approaches possess an excellent biocompatibility.

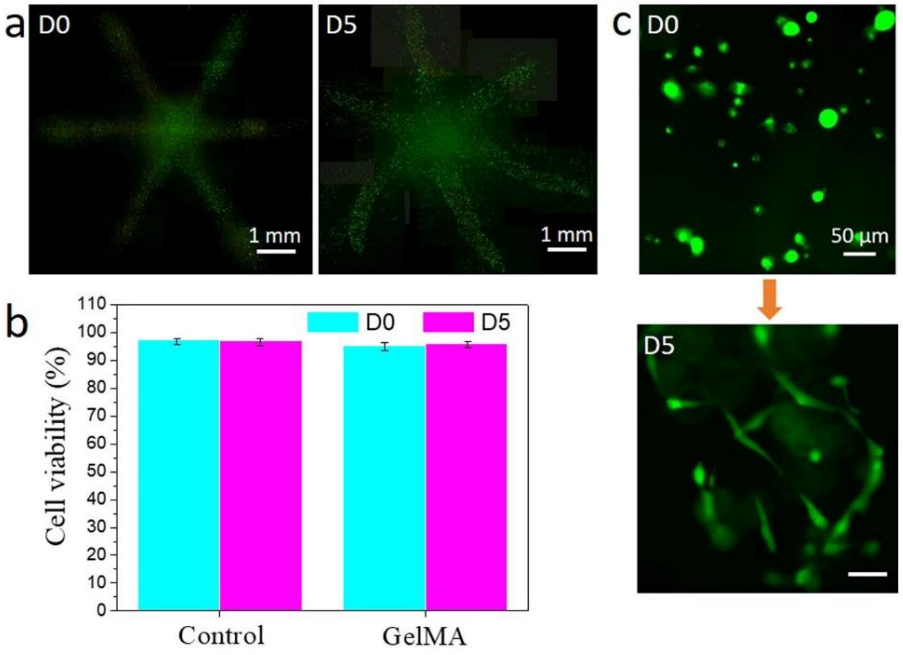


**Fig. 9**. Cell viability for submerged printing: (a) merged fluorescent images for the cells on the printed structure; (b) cell viability of the bioprinted GelMA structure and the control; (c) representative images to highlight cell morphologies.

## 4. Discussion

MC is derived from the naturally occurring polysaccharide cellulose. The presence of the methoxy-substitution of some hydroxyl groups in the main β-glucose chain decrease the intermolecular hydrogen bonding making MC a water-soluble polymer [37, 38]. After adding MC

to Alg hydrogel, the viscosity of this blend can be improved significantly due to the hydrogen-bonding between carboxyl groups (-COOH) and hydrophilic hydroxy groups (-OH), the hydrophobic interaction between MC molecules, and the creation of a semi-interpenetrating network-like structure between Alg and MC [39].

The highly viscous Alg/MC hydrogel blend can be used as a self-support material for extrusion-based printing as it demonstrated excellent shape fidelity and stackability [25, 26]. On the basis of rheological test (**Fig. S1**, Supporting Information), the Alg/MC blend presented the shear-thinning and thixotropic properties which are desirable for the extrusion-based printing. Additionally, Alg/MC could be also selected as a supporting material. The movement of the nozzle through this Alg/MC hydrogel will lead to a decreased viscosity of the nearby Alg/MC hydrogel due to its shear thinning property, which could help the nozzle easily move through the support material Alg/MC. Subsequently, the shear-reduced viscosity of Alg/MC could be rapidly recovered to support the other suspended hydrogel after removing the shear force due to the thixotropic property of Alg/MC. Moreover, the Alg/MC has an ultra-high printability but low bioactivity [6, 40-42], while GelMA is a popular bioactive hydrogel but has poor stackability. In this study, the individual characteristics of this hydrogel pair were combined synergistically.

This study proposed two approaches (non-submerged and submerged printing) for bioprinting of 3D complex cell-laden structures with the hydrogel pair Alg/MC and GelMA. For the non-submerged approach, the highly viscous Alg/MC hydrogel blend and the cell-GelMA mixture were printed alternately to create the structures with living cells. The highly viscous Alg/MC can be printed first to obtain the base layer, which can provide the support to the next cell-GelMA layer, which could not maintain its 3D-printed shape without UV curing. For the submerged approach, the cell-GelMA mixture was embedded in the Alg/MC, which was used as a temporary supporting material during printing. This approach can be used to print complex structures with increasing complexity which could not be obtained through the first approach. For both approaches, the printed structures were exposed to UV light only once after printing to strengthen them. However,

each printed GelMA layer without the treatment of UV curing might collapse and could not maintain its shape when being stacked on top. Thus, before the UV curing, the electrostatic interaction between Alg/MC and GelMA hydrogels would be an efficient way to prevent GelMA from collapsing and form stable structures during the printing process.

According to the literature [43, 44], the gelling temperature of MC-based hydrogel could be influenced by concentration and molecular weight of MC as well as salt content. In this study, the molecular weight of MC is 88 kDa. However, MC-based gel was not expected to form gel at 37 $^{o}$C or below [44]. Thus, MC could release from the printed structure at 37 $^{o}$C. Meanwhile, some study pointed that steric hindrance leads to a slow diffusion rate of the MC (MW of 88 kDa) within the Alg network [25, 45]. For the Alg/MC-GelMA constructs obtained through the non-submerged approach, it can well maintain its shape for 15 days. A slow degradation rate of MC can be assumed as the good structural integrity of Alg/MC-GelMA was observed.

There are obvious advantages of employing these two proposed approaches with the hydrogel pair for bioprinting. Firstly, the proposed approaches were successful in overcoming the limitation posed by the conventional methodology of utilizing GelMA for printing where UV curing is applied for each layer. On contrary, in this work, the final printed structures were exposed to UV light once only (e.g., 10 s in the UV flood). Secondly, the barrier of printing complex structures was removed by using the submerged approach with the hydrogel pair Alg/MC and GelMA while earlier only limited simple hydrogel structures (e.g., lattices) can be printed using traditional bioprinting strategies. Finally, GelMA possess three functions here: a channel for delivering cells for printing, an agent for promoting cell adhesion and a medium for providing the positive charged ions to have electrostatic interactions with the negatively charged Alg/MC. The proposed approaches of using GelMA for delivering cells could overcome the drawbacks of solely printing of one hydrogel (e.g., high stress on the viscous cell-laden hydrogel) [33, 46]. GelMA contains peptide arginine-glycine-aspartic acid, which could provide the binding sites for cell adhesion [47]. GelMA used in this study exhibited a cationic nature while Alg contains negatively charged carboxylate groups, which

can form electrostatic interactions with the cations [48]. Thus, the polyelectrolyte complexes between Alg/MC and GelMA could stabilize the printed structures during the 3D printing process.

As discussed previously, the main challenge lies in the fabrication of a soft hydrogel into a 3D structure as each printed layer should maintain its shape and even support the upper layers on top of it. Here, complex structures with living cells were successfully printed through using the non-submerged and submerged printing with the aid of a hydrogel pair. Cell viability of the printed structures maintained above 93% for 5 days of culturing. The elongation of cells can also be observed in the printed structures. Alg/MC blend and GelMA are easily prepared, inexpensive and biocompatible, which can broaden the application of such materials and approaches in the field of 3D bioprinting.

## 5. Conclusions

Here, non-submerged and submerged printing approaches were proposed for fabrication of complex hydrogel structures with the hydrogel pair Alg/MC and GelMA. Each approach demonstrates its own advantages for bioprinting. For the non-submerged approach, a highly viscous hydrogel that can rapidly solidify (e.g., Alg/MC) was used to provide support for the other hydrogel with a low viscosity (e.g., cell-laden GelMA). Furthermore, alternately printing of two oppositely charged hydrogels Alg/MC and GelMA could overcome the disadvantages of solely printing one hydrogel (e.g., high stress on the viscous cell-laden hydrogel). For the submerged approach, the cell-laden GelMA was printed in the viscous Alg/MC, which provided temporary support for the GelMA. This approach can be utilized for fabrication of complex structures rather than simpler ones (i.e. grids).

For both approaches, the obtained structures with living cells were exposed to UV light only once after printing, which overcomes the limitations of utilizing GelMA for bioprinting. In this study, GelMA possess three functions: a channel for delivering cells for printing, a medium for

providing the positive charged ions to have electrostatic interactions with the negatively charged Alg/MC, and an agent for promoting cell adhesion. Based on the above findings, this promising pair of bioinks, together with the aid of these two proposed printing approaches, opens up many opportunities in 3D printing, including the broadening of hydrogel candidates list for bioprinting; expand the great potential for the fabrication of complex hydrogel structures with living cells in the field of 3D bioprinting.

**Acknowledgments**

The authors acknowledge the financial support from the Nanyang Technological University, Singapore and the National Research Foundation Medium Sized Center, Singapore through the Marine and Offshore Programme.

**References**

[1] C.K. Chua, C.H. Wong, W.Y. Yeong, Standards, Quality Control, and Measurement Sciences in 3D Printing and Additive Manufacturing, Elsevier Academic Press Inc, San Diego, 2017.
[2] C.K. Chua, K.F. Leong, 3D Printing and Additive Manufacturing : Principles and Applications, 5th edition, World Scientific, Singapore, 2017.
[3] P. Zhuang, A.X. Sun, J. An, C.K. Chua, S.Y. Chew, 3D Neural Tissue Models: From Spheroids to Bioprinting, Biomaterials 154 (2018) 113-133.
[4] S.V. Murphy, A. Atala, 3D Bioprinting of Tissues and Organs, Nature Biotechnology 32(8) (2014) 773-785.
[5] H. Li, C. Tan, L. Li, Review of 3D Printable Hydrogels and Constructs, Materials & Design 159 (2018) 20-38.
[6] Z.J. Wu, X. Su, Y.Y. Xu, B. Kong, W. Sun, S.L. Mi, Bioprinting Three-Dimensional Cell-Laden Tissue Constructs with Controllable Degradation, Scientific Reports 6 (2016).
[7] Q. Gao, Y. He, J.Z. Fu, A. Liu, L. Ma, Coaxial Nozzle-Assisted 3D Bioprinting with Built-in Microchannels for Nutrients Delivery, Biomaterials 61 (2015) 203-215.
[8] S.F. Yang, H.Y. Yang, X.P. Chi, J.R.G. Evans, I. Thompson, R.J. Cook, P. Robinson, Rapid Prototyping of Ceramic Lattices for Hard Tissue Scaffolds, Materials & Design 29(9) (2008) 1802-1809.
[9] Y.J. Tan, X.P. Tan, W.Y. Yeong, S.B. Tor, Hybrid Microscaffold-Based 3D Bioprinting of Multi-Cellular Constructs with High Compressive Strength: A New Biofabrication Strategy, Scientific Reports 6 (2016).
[10] C. Li, A. Faulkner-Jones, A.R. Dun, J. Jin, P. Chen, Y.Z. Xing, Z.Q. Yang, Z.B. Li, W.M. Shu, D.S. Liu, R.R. Duncan, Rapid Formation of a Supramolecular Polypeptide-DNA Hydrogel for In Situ

Three-Dimensional Multilayer Bioprinting, Angewandte Chemie-International Edition 54(13) (2015) 3957-3961.
[11] F. Guillemot, A. Souquet, S. Catros, B. Guillotin, J. Lopez, M. Faucon, B. Pippenger, R. Bareille, M. Remy, S. Bellance, P. Chabassier, J.C. Fricain, J. Amedee, High-Throughput Laser Printing of Cells and Biomaterials for Tissue Engineering, Acta Biomaterialia 6(7) (2010) 2494-2500.
[12] N. Jones, Science in Three Dimensions: The Print Revolution, 487 (2012) 22-23.
[13] D.M. Kirchmajer, R. Gorkin, M.I.H. Panhuis, An Overview of The Suitability of Hydrogel-Forming Polymers for Extrusion-Based 3D-Printing, Journal of Materials Chemistry B 3(20) (2015) 4105-4117.
[14] H. Li, S. Liu, L. Li, Rheological Study on 3D Printability of Alginate Hydrogel and Effect of Graphene Oxide, International Journal of Bioprinting 2(2) (2016) 54-66.
[15] J. Leppiniemi, P. Lahtinen, A. Paajanen, R. Mahlberg, S. Metsa-Kortelainen, T. Pinornaa, H. Pajari, I. Vikholm-Lundin, P. Pursula, V.P. Hytonen, 3D-Printable Bioactivated Nanocellulose-Alginate Hydrogels, Acs Applied Materials & Interfaces 9(26) (2017) 21959-21970.
[16] A. Lode, M. Meyer, S. Bruggemeier, B. Paul, H. Baltzer, M. Schropfer, C. Winkelmann, F. Sonntag, M. Gelinsky, Additive Manufacturing of Collagen Scaffolds by Three-Dimensional Plotting of Highly Viscous Dispersions, Biofabrication 8(1) (2016).
[17] T. Zehnder, B. Sarker, A.R. Boccaccini, R. Detsch, Evaluation of an Alginate-Gelatine Crosslinked Hydrogel for Bioplotting, Biofabrication 7(2) (2015).
[18] Y. Huang, S. Onyeri, M. Siewe, A. Moshfeghian, S.V. Madihally, In Vitro Characterization of Chitosan-Gelatin Scaffolds for Tissue Engineering, Biomaterials 26(36) (2005) 7616-7627.
[19] Y.X. Xu, D.D. Xia, J.M. Han, S.P. Yuan, H. Lin, C. Zhao, Design and Fabrication of Porous Chitosan Scaffolds with Tunable Structures and Mechanical Properties, Carbohydrate Polymers 177 (2017) 210-216.
[20] L. Geng, W. Feng, D.W. Hutmacher, Y.S. Wong, H.T. Loh, J.Y.H. Fuh, Direct Writing of Chitosan Scaffolds Using A Robotic System, Rapid Prototyping Journal 11(2) (2005) 90-97.
[21] T.J. Hinton, Q. Jallerat, R.N. Palchesko, J.H. Park, M.S. Grodzicki, H.J. Shue, M.H. Ramadan, A.R. Hudson, A.W. Feinberg, Three-Dimensional Printing of Complex Biological Structures by Freeform Reversible Embedding of Suspended Hydrogels, Science Advances 1(9) (2015).
[22] I. Donderwinkel, J.C.M. van Hest, N.R. Cameron, Bio-Inks for 3D Bioprinting: Recent Advances and Future Prospects, Polymer Chemistry 8(31) (2017) 4451-4471.
[23] J.E. Kim, S.H. Kim, Y. Jung, Current Status of Three-Dimensional Printing Inks for Soft Tissue Regeneration, Tissue Engineering and Regenerative Medicine 13(6) (2016) 636-646.
[24] W. Schuurman, P.A. Levett, M.W. Pot, P.R. van Weeren, W.J.A. Dhert, D.W. Hutmacher, F.P.W. Melchels, T.J. Klein, J. Malda, Gelatin-Methacrylamide Hydrogels as Potential Biomaterials for Fabrication of Tissue-Engineered Cartilage Constructs, Macromolecular Bioscience 13(5) (2013) 551-561.
[25] K. Schutz, A.M. Placht, B. Paul, S. Bruggemeier, M. Gelinsky, A. Lode, Three-Dimensional Plotting of A Cell-Laden Alginate/Methylcellulose Blend: Towards Biofabrication of Tissue Engineering Constructs with Clinically Relevant Dimensions, Journal of Tissue Engineering and Regenerative Medicine 11(5) (2017) 1574-1587.
[26] H. Li, Y.J. Tan, K.F. Leong, L. Li, 3D Bioprinting of Highly Thixotropic Alginate/Methylcellulose Hydrogel with Strong Interface Bonding, Acs Applied Materials & Interfaces 9(23) (2017) 20086-20097.
[27] Y.F. Jin, C.C. Liu, W.X. Chai, A. Compaan, Y. Huang, Self-Supporting Nanoclay as Internal Scaffold Material for Direct Printing of Soft Hydrogel Composite Structures in Air, Acs Applied Materials & Interfaces 9(20) (2017) 17457-17466.

[28] T.J. Hinton, A. Hudson, K. Pusch, A. Lee, A.W. Feinberg, 3D Printing PDMS Elastomer in A Hydrophilic Support Bath via Freeform Reversible Embedding, Acs Biomaterials Science & Engineering 2(10) (2016) 1781-1786.
[29] H.Z. Ding, R.C. Chang, Printability Study of Bioprinted Tubular Structures Using Liquid Hydrogel Precursors in a Support Bath, Applied Sciences-Basel 8(3) (2018).
[30] A.G. Tabriz, M.A. Hermida, N.R. Leslie, W.M. Shu, Three-Dimensional Bioprinting of Complex Cell Laden Alginate Hydrogel Structures, Biofabrication 7(4) (2015).
[31] J. Malda, J. Visser, F.P. Melchels, T. Jüngst, W.E. Hennink, W.J.A. Dhert, J. Groll, D.W. Hutmacher, 25th Anniversary Article: Engineering Hydrogels for Biofabrication, Advanced Materials 25(36) (2013) 5011-5028.
[32] J.W. Nichol, S.T. Koshy, H. Bae, C.M. Hwang, S. Yamanlar, A. Khademhosseini, Cell-Laden Microengineered Gelatin Methacrylate Hydrogels, Biomaterials 31(21) (2010) 5536-5544.
[33] H. Li, Y.J. Tan, S. Liu, L. Li, Three-Dimensional Bioprinting of Oppositely Charged Hydrogels with Super Strong Interface Bonding, Acs Applied Materials & Interfaces 10(13) (2018) 11164-11174.
[34] L.L. Ouyang, R. Yao, Y. Zhao, W. Sun, Effect of Bioink Properties on Printability and Cell Viability for 3D Bioplotting of Embryonic Stem Cells, Biofabrication 8(3) (2016).
[35] Y.J. Tan, K.F. Leong, J. An, K.S. Chian, X.P. Tan, W.Y. Yeong, Fabrication and in Vitro Analysis of Tubular Scaffolds by Melt-Drawing for Esophageal Tissue Engineering, Materials Letters 159 (2015) 424-427.
[36] S.K. Samal, M. Dash, S. Van Vlierberghe, D.L. Kaplan, E. Chiellini, C. van Blitterswijk, L. Moroni, P. Dubruel, Cationic Polymers and Their Therapeutic Potential, Chemical Society Reviews 41(21) (2012) 7147-7194.
[37] L. Li, P.M. Thangamathesvaran, C.Y. Yue, K.C. Tam, X. Hu, Y.C. Lam, Gel Network Structure of Methylcellulose in Water, Langmuir 17(26) (2001) 8062-8068.
[38] L. Li, Thermal Gelation of Methylcellulose in Water: Scaling and Thermoreversibility, Macromolecules 35(15) (2002) 5990-5998.
[39] H.F. Liang, M.H. Hong, R.M. Ho, C.K. Chung, Y.H. Lin, C.H. Chen, H.W. Sung, Novel Method Using a Temperature-Sensitive Polymer (Methylcellulose) to Thermally Gel Aqueous Alginate as a pH-Sensitive Hydrogel, Biomacromolecules 5(5) (2004) 1917-1925.
[40] K.Y. Lee, D.J. Mooney, Alginate: Properties and Biomedical Applications, Progress in Polymer Science 37(1) (2012) 106-126.
[41] J.A. Rowley, G. Madlambayan, D.J. Mooney, Alginate Hydrogels as Synthetic Extracellular Matrix Materials, Biomaterials 20(1) (1999) 45-53.
[42] R. Suntornnond, J. An, C.K. Chua, Bioprinting of Thermoresponsive Hydrogels for Next Generation Tissue Engineering: A Review, Macromolecular Materials and Engineering 302(1) (2017).
[43] Y. Xu, C. Wang, K.C. Tam, L. Li, Salt-Assisted and Salt-Suppressed Sol−Gel Transitions of Methylcellulose in Water, Langmuir 20(3) (2004) 646-652.
[44] S. Thirumala, J. Gimble, R. Devireddy, Methylcellulose Based Thermally Reversible Hydrogel System for Tissue Engineering Applications, Cells 2 (2013) 460-75.
[45] N. Wang, G. Adams, L. Buttery, F. Falcone, S. Stolnik, Alginate encapsulation technology supports embryonic stem cells differentiation into insulin-producing cells, Journal of biotechnology 144 (2009) 304-12.
[46] H. Li, Y.J. Tan, L. Li, A Strategy for Strong Interface Bonding by 3D Bioprinting of Oppositely Charged kappa-carrageenan and Gelatin Hydrogels, Carbohydrate Polymers 198 (2018) 261-269.

[47] S. Sakai, K. Hirose, K. Taguchi, Y. Ogushi, K. Kawakami, An Injectable, in Situ Enzymatically Gellable, Gelatin Derivative for Drug Delivery and Tissue Engineering, Biomaterials 30(20) (2009) 3371-3377.
[48] H. Gudapati, M. Dey, I. Ozbolat, A Comprehensive Review on Droplet-Based Bioprinting: Past, Present and Future, Biomaterials 102 (2016) 20-42.